Chemical Research in Toxicology

Article

Cite This: Chem. Res. Toxicol. 2017, 30, 2023-2032

pubs.acs.org/crt

Mechanism of Error-Free DNA Replication Past Lucidin-Derived DNA Damage by Human DNA Polymerase κ

Oliver P. Yockey,[†,¶] Vikash Jha,[§,¶] Pratibha P. Ghodke,[⊥,¶] Tianzuo Xu,[†] Wenyan Xu,[†] Hong Ling,[*,§] P. I. Pradeepkumar,[*,⊥] and Linlin Zhao[*,†,‡]

[†]Department of Chemistry and Biochemistry and [‡]Science of Advanced Materials Program, Central Michigan University, Mount Pleasant, Michigan 48859, United States

[§]Department of Biochemistry, Schulich School of Medicine & Dentistry, University of Western Ontario, London, Ontario N6A 5C1, Canada

[⊥]Department of Chemistry, Indian Institute of Technology Bombay, Mumbai 400076, India

Supporting Information

ABSTRACT: DNA damage impinges on genetic information flow and has significant implications in human disease and aging. Lucidin-3-*O*-primeveroside (LuP) is an anthraquinone derivative present in madder root, which has been used as a coloring agent and food additive. LuP can be metabolically converted to genotoxic compound lucidin, which subsequently forms lucidin-specific N^2-2′-deoxyguanosine (N^2-dG) and N^6-2′-deoxyadenosine (N^6-dA) DNA adducts. Lucidin is mutagenic and carcinogenic in rodents but has low carcinogenic risks in humans. To understand the molecular mechanism of low carcinogenicity of lucidin in humans, we performed DNA replication assays using site-specifically modified oligodeoxynucleotides containing a structural analogue (LdG) of lucidin-N^2-dG DNA adduct and determined the crystal structures of DNA polymerase (pol) κ in complex with LdG-bearing DNA and an incoming nucleotide. We examined four human pols (pol η, pol ι, pol κ, and Rev1) in their efficiency and accuracy during DNA replication with LdG; these pols are key players in translesion DNA synthesis. Our results demonstrate that pol κ efficiently and accurately replicates past the LdG adduct, whereas DNA replication by pol η, pol ι is compromised to different extents. Rev1 retains its ability to incorporate dCTP opposite the lesion albeit with decreased efficiency. Two ternary crystal structures of pol κ illustrate that the LdG adduct is accommodated by pol κ at the enzyme active site during insertion and postlesion-extension steps. The unique open active site of pol κ allows the adducted DNA to adopt a standard B-form for accurate DNA replication. Collectively, these biochemical and structural data provide mechanistic insights into the low carcinogenic risk of lucidin in humans.

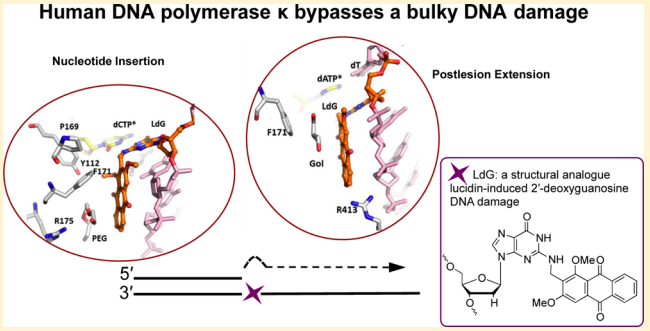

INTRODUCTION

The genetic material DNA is susceptible to numerous endogenous and exogenous chemicals. The chemically modified DNA, often referred to as DNA adduct or DNA lesion, has important biological implications and has been used as biomarkers in molecular epidemiology studies.[1−4] Unrepaired DNA lesions can block DNA replication, cause mutations and cell death, and contribute to pathogenesis.[5] To ensure continuous DNA duplication, specialized DNA polymerases (pols) are utilized to incorporate one or a few nucleotides past a noncanonical DNA structure.[6,7] This DNA damage tolerance mechanism, known as translesion synthesis (TLS), is conserved from bacteria to humans.[8] Notably, TLS is error-prone and plays a vital role in DNA damage-induced mutations and disease etiology.[5,9] In humans, pol η, pol ι, pol κ, Rev1, and pol ζ are major TLS pols, of which each has a unique DNA damage bypass and fidelity profile.[6,7] For example, human pol κ is known for its capability of performing error-free DNA replication to bypass the N^2-dG DNA adduct formed by carcinogen benzo[*a*]pyrene-7,8-dihydrodiol-9,10-epoxide (BPDE) *in vitro* and inside cells.[10,11]

Madder color, extracted from *Rubia tinctrum L.* (madder root), has been used as a dyeing agent since ancient times. Madder root has also been used as an herbal medicine for treating kidney and bladder stones[12,13] and urinary disorders.[14] In Japan and Korea, madder color had been used as a natural food colorant and additive, and such use was banned in 2004 in both countries due to its toxicity in experimental animals.[15−17] In rats, madder root exerts carcinogenicity;[17,18] however, in humans madder root is classified as Group 3 (i.e., not classifiable as to its carcinogenicity to humans) by the

Special Issue: DNA Polymerases: From Molecular Mechanisms to Human Disease

Received: August 14, 2017
Published: October 3, 2017

DOI: 10.1021/acs.chemrestox.7b00227
Chem. Res. Toxicol. 2017, 30, 2023−2032

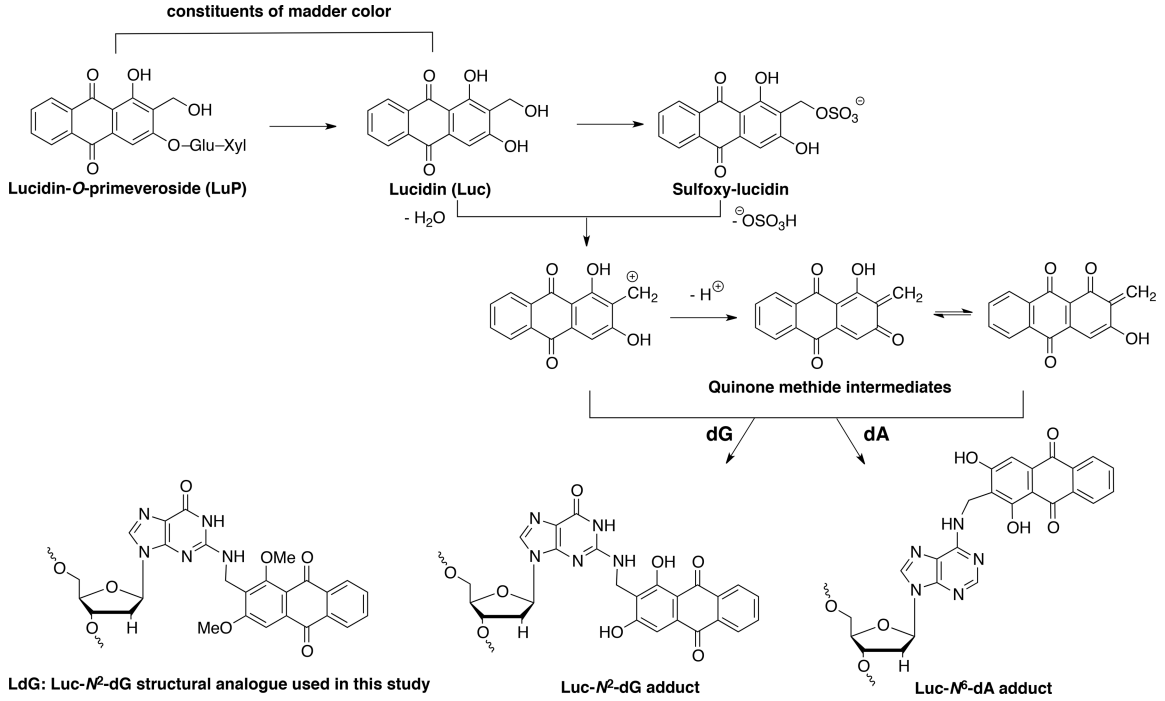

Figure 1. Metabolic activation of lucidin-*O*-primeveroside and lucidin, and formation of ludicin-derived DNA adducts. The structure of synthetic analogue (LdG) of lucidin-N^2-2′-deoxyguanosine adduct is shown.

International Agency for Research on Cancer.[19] The reason for the low carcinogenic risk of lucidin in humans remains unclear.

Madder root contains various hydroxyanthraquinones, such as lucidin, alizarin, and their glycoside derivatives such as lucidin-*O*-primeveroside (LuP).[19] LuP and lucidin can be metabolically activated to form quinone methide intermediates that are reactive toward DNA (Figure 1). Lucidin is a potent carcinogen that affects the kidney and liver in rats.[17] Lucidin-specific N^2-2′-deoxyguanosine (N^2-dG) and N^6-2′-deoxyadenosine (N^6-dA) DNA adducts have been identified *in vitro* and in LuP-treated rats.[20,21] *In vivo* mutation assays have shown that lucidin induces G to T and A to T transversion and A to G transition mutations in rats.[18,22] Therefore, LuP is considered as a major contributor to the madder root-induced carcinogenicity in rats.

The biological significance and potential association with animal carcinogenicity of lucidin-N^2-dG and lucidin-N^6-dA adducts remain elusive. Because these DNA modifications can interfere with the Watson−Crick hydrogen bonding, they are likely to be replication-blocking or mutagenic. To better understand the miscoding property of lucidin-derived DNA damage in humans, we developed a method to site-specifically incorporate a structural analogue N^2-methyl-(1,3-dimethoxyanthraquinone)-deoxyguanosine (LdG) of lucidin-N^2-dG (Figure 1) into DNA oligomers.[23] The structural analogue was used due to unsuccessful attempts to synthesize 2-(aminomethyl)-1,3-diacetoxyanthraquinone, an acetyl protected lucidin amine required to assemble the N^2-dG nucleoside via Buchwald-Hartwig coupling.[23] *In vitro* DNA replication assays using model *Escherichia coli* DNA polymerase I Klenow fragment revealed that the LdG lesion inhibited primer extension and induced misincorporations.[23] Herein, we unravel the miscoding property of LdG with key human TLS DNA polymerases and describe the mechanism of error-free DNA bypass by pol κ using biochemical and structural approaches. We discover that DNA replication past LdG is mainly error-free; in particular, human pol κ bypasses LdG efficiently and accurately. Three other TLS pols (pol η, pol ι, and Rev1) showed different degrees of attenuation in DNA replication fidelity and efficiency when bypassing LdG. To determine the structural basis of pol κ-catalyzed bypass, we solved two high-resolution X-ray crystal structures of pol κ:LdG-DNA:dNTP, correlating to the insertion (opposite the lesion) and extension steps during lesion bypass. Pol κ accommodates LdG in both structures and maintains productive conformations during TLS. Taken together, this work provides the first mechanistic explanation concerning the low carcinogenic risk of lucidin in humans and sheds light on the versatility of pol κ in replicating past the N^2-dG DNA damage.

MATERIALS AND METHODS

Materials. Unlabeled dNTPs, T4 polynucleotide kinase, and uracil DNA glycosylase (UDG) were from New England Biolabs (Ipswich, MA). [γ-^{32}P]ATP (specific activity of 3000 Ci/mmol) was from PerkinElmer (Waltham, MA). All other commercial chemicals were from Sigma-Aldrich (St. Louis, MO) or Research Products International (Mt Prospect, IL) and were of the highest quality available. Unmodified DNA oligodeoxynucleotides were synthesized and PAGE-purified by Integrated DNA Technologies (Coralville, IA). DNA oligodeoxynucleotides containing a site-specifically modified LdG adduct were synthesized and purified as described previously (see Supporting Information for details).[23] The catalytic fragments of human Y-family DNA polymerases pol ι (1−420),[24] pol η (1−432),[25] pol κ (19−526),[26] and REV1 (330−833)[27] were purified as described previously.

Primer Extension Assays. A 15- or 16-mer primer was 5′ [γ-^{32}P]ATP end-labeled and annealed to a 50-mer unmodified or LdG-bearing oligomer; sequences are shown in Table S1 of the Supporting Information. Primer-extension assays were performed and analyzed as previously described.[28] Reaction conditions are specified as follows. Full-length extension assays were performed at 37 °C using 80 nM primer-template DNA, 80 nM DNA polymerase, four dNTPs at their physiological concentrations[29] (i.e., 10 μM for dGTP and 40 μM for dATP, dCTP, and dTTP), 4% (v/v) glycerol, 5 mM DTT, 50 mM

DOI: 10.1021/acs.chemrestox.7b00227
Chem. Res. Toxicol. 2017, 30, 2023−2032

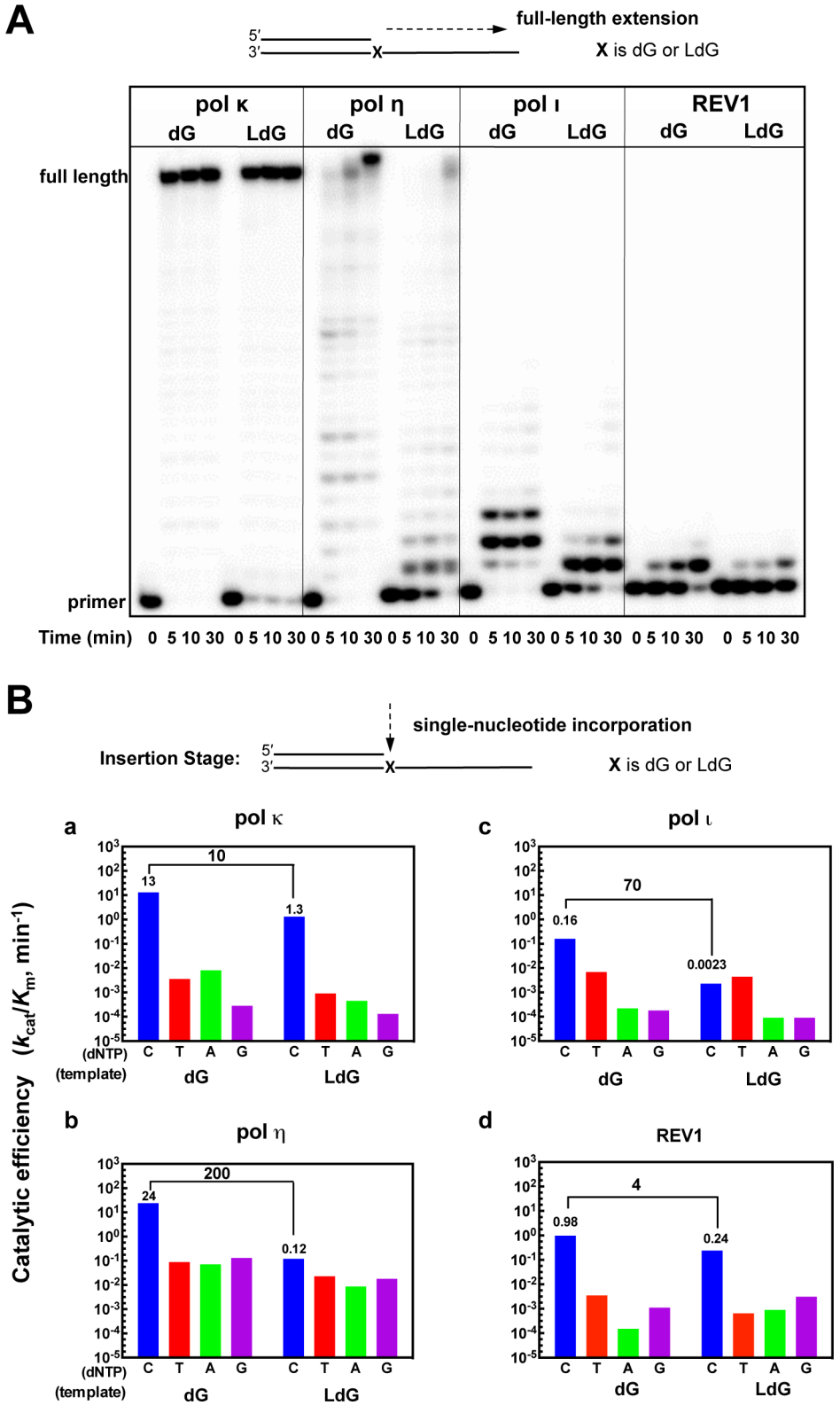

Figure 2. Translesion DNA synthesis by human DNA polymerases κ, η, ι, or Rev1 with unmodified or LdG-containing DNA substrate. Reaction conditions are described in the Materials and Methods section. (A) Primer extension reactions in the presence of all four dNTPs at their physiological concentrations (i.e., 10 μM for dGTP and 40 μM for dATP, dCTP, and dTTP). (B) Catalytic efficiencies of individual dNTPs opposite unmodified dG or LdG adduct. Enzyme kinetic parameters are shown in the Supporting Information Table S2. Changes in catalytic efficiency relative to a native base pair were calculated from $(k_{cat}/K_{m,dCTP})_{unmodified}/(k_{cat}/K_{m,dCTP})_{LdG}$ and indicated as x-fold decrease.

NaCl, 5 mM $MgCl_2$, and 100 μg/mL bovine serum albumin (BSA) in 50 mM Tris-HCl (pH 7.4 at 25 °C). Single-nucleotide incorporations were conducted under the same condition except that 80−400 nM primer-template DNA, 0.5−20 nM DNA polymerase, and varying concentrations of a single dNTP were used to keep the reaction under steady-state kinetic conditions. Gels were imaged using a phosphor-

DOI: 10.1021/acs.chemrestox.7b00227
Chem. Res. Toxicol. 2017, 30, 2023−2032

imaging system (GE Healthcare, Typhoon FLA7000) and analyzed with ImageQuant software. Data were fit to the Michaelis−Menten equation using Prism software (GraphPad, San Diego, CA).

NanoLC−MS/MS Analysis of Primer-Extension Products by Pol κ. A 15-mer primer 5′-TAATGGCTAACGC(dU)T-3′ was annealed to an unmodified or an LdG-containing 29-mer oligomer at a 1:1.2 molar ratio (template sequence shown in Table S1). The pol κ-catalyzed polymerization was allowed for 3 h in the presence of 2 μM DNA complex and 0.3 μM pol κ in a total volume of 50 μL (other reaction components are the same as those used in full-length primer extension assays) at 37 °C. Reactions were quenched with 10 mM EDTA (final concentration) followed by UDG digestion overnight at 37 °C. Phenol/chloroform extraction was used to purify DNA oligomers, which were subsequently cleaved with hot piperidine (0.25 M piperidine at 90 °C for 1 h). Reaction products were purified with a C18 SampliQ solid-phase extraction cartridge (Agilent Technologies). The fractions containing oligomer were dried under vacuum and suspended in 30 μL of chromatography mobile phase A *vide infra*.

NanoLC−MS/MS analysis was performed on a nanoAcquity ultraperformance liquid chromatography system (Waters Corp.) connected to a Finnigan LTQ XL mass spectrometer (Thermo Scientific Corp.). Data were collected under negative ionization mode. The column used was a PicoChip column (75 μm ID, 105 mm bed length and a 15 μm tip, New Objective, Woburn, MA) packed with Reprosil-PUR C18 (3 μm, 120 Å) chromatography media. Chromatography mobile phase A was 400 mM 1,1,1,3,3,3-hexafluoro-2-propanol in water (pH adjusted to 7.0 with triethylamine) and mobile phase B was methanol. The following gradient program was used at a flow rate of 250 nL/min: 0−5 min, maintained at 95% A/5% B (v/v); 5−45 min, linear gradient to 30% B (v/v); 45−55 min, linear gradient to 50% B; 55−60 min, hold at 50% B; 60−105 min, linear gradient to 5% B; 105−130 min, hold at 5% B to re-equilibrium the column. A 5 μL aliquot was injected onto the column. Nanoelectrospray conditions were as follows: ionization voltage 3 kV, capillary temperature 300 °C, capillary voltage −45 V, tube lens voltage −110 V. MS/MS conditions were as follows: normalized collision energy 40%, activation Q 0.250, and activation time 30 ms. Product ion spectra were acquired over the range m/z 300−1800. The most abundant species was used for CID analysis. Theoretical fragmentated ions were calculated using the Mongo Oligo mass calculator version 2.06 (hosted by the State University of New York at Albany).[30] The relative yield of extension products was determined based on the integrated peak areas in extracted ion chromatograms, which were set to extract multiple species with different charged states. The sum of peak area ratios of all products/residual primer was set to 100% for each reaction.

Crystallization of DNA:Pol κ:dNTP Ternary Complexes. Human pol κ protein containing residues 1−526 with 6xHis-tag on the N-terminal was overexpressed and purified as described previously.[31] The 22-mer template 5′-ATGG*CTGAT-CCGCGCGGATCAG-3′ was used to cocrystallize the insertion complex, and 5′-CTATG*TCGATCCGCGGATCGAC-3′ was used to cocrystallize the extension complex (G* denotes LdG). These DNA substrates are self-annealing DNA oligomers; their sequences are designed to avoid hairpin formation and maximize the stability of primer-template DNA. The self annealing DNA was incubated with pol κ in a 1.2:1 ratio in presence of 10 mM $MgCl_2$. The ternary complexes of pol κ with DNA containing LdG and an incoming nucleotide were prepared as previously described.[31,32] Briefly, pol κ was mixed with primer-template DNA and 2 mM of nonhydrolyzable nucleotide dCMPNPP (2′-deoxycytidine-5′-[(α,β)-imido] triphosphate, hereafter termed dCTP*) for the insertion complex or dAMPNPP (2′-deoxyadenosine-5′-[(α,β)-imido] triphosphate, hereafter termed dATP*) for the extension complex. The complex mixture was incubated at room temperature for 30 min before setting up crystallization. The ternary complex cocrystals were grown by hanging drop vapor diffusion method at 22 °C with a well solution containing 25−30% PEG400 and 0.1−0.2 M ammonium nitrate. To obtain good quality crystals, drops were streak seeded several times. The pol κ:DNA cocrystals were picked from the drop, cryoprotected with 35% PEG400, 0.2 M ammonium nitrate and 20% ethylene glycol and then flash frozen in liquid nitrogen for data collection. X-ray diffraction data were collected at the beamline 24-ID-E operated by the Northeastern Collaborative Access Team (NE-CAT) at the Advanced Photon Source. Diffraction data were processed using iMolsfm and Scala in the CCP4 suite.[33] Structure refinement was performed using REFMAC5.[34] Model building and inspection was performed in Coot[35] and the crystallographic figures were generated using the molecular graphics program PyMOL.[36]

RESULTS AND DISCUSSION

Pol κ Efficiently Replicates Past LdG Adduct. The lucidin-N^2-dG adduct is a major adduct observed in reactions between the reactive metabolites of LuP and DNA *in vitro* and in the kidneys and livers of LuP-treated rats.[20,21] The objectives of this study are (1) to decipher the miscoding pattern of lucidin-N^2-dG lesion during human TLS and (2) to gain mechanistic insight into such processes. To this end, we used our recently developed method to synthesize site-specifically modified oligodeoxynucleotides containing an LdG analogue.[23] Using steady-state kinetic analysis, we determined the bypass capability, dNTP incorporation efficiency, and DNA replication fidelity of translesion and postlesion syntheses for human TLS pols, η, ι, κ, and Rev1. These pols are Y-family enzymes in DNA damage bypass. The DNA damage bypass occurs when the DNA replication is blocked by a DNA adduct or a noncanonical DNA structure, and involves several polymerase-switching processes to unload a replicative DNA polymerase and recruit one or more TLS pols to rescue a stalled replication fork.[37] In addition, translesion synthesis can also be used to fill postreplicative gaps.[38−40] To first qualitatively assess the DNA bypass abilities of different TLS DNA polymerases, a reconstituted system was used containing an LdG-harboring primer-template DNA (or an unmodified DNA), a TLS pol, and four dNTPs at physiological concentrations. The extent of primer-extension is an indication of bypass capability of a particular pol. As shown in Figure 2A, relative to an undamaged DNA, LdG had the least impact on the DNA replication activity of pol κ. Pol κ was capable of bypassing LdG with high enzymatic activity, resulting in approximately 71% of the products extended to full-length in a 5 min reaction, which is similar to the yield obtained with the undamaged substrate. This observation is consistent with the known property of pol κ in tolerating N^2-dG DNA adducts.[10,31,41−44] On the other hand, pol η and pol ι primarily produced one-nucleotide-extension products with the LdG-containing substrate (Figure 2A). Pol η weakly bypassed LdG and generated 16% full-length products in a 30 min reaction. Pol ι barely produced any products other than the products with one-nucleotide extension, in keeping with the low processivity of this enzyme.[45] Rev1, a dCTP transferase, is able to perform dNTP incorporation with the LdG-substrate, albeit with lower activity relative to the unmodified DNA. Together, these results demonstrate that the bulky LdG exhibits a minimal impact on the dNTP-incorporation activity of pol κ and a minor impact on that of Rev1, whereas the same lesion compromises the enzyme activities of pol η and pol ι.

dNTP Incorporation Opposite LdG Adduct Is Mainly Error-Free. To understand the specificity of dNTP incorporation opposite LdG, we determined enzyme kinetic parameters, such as Michaelis constant (K_m), turnover number (k_{cat}), catalytic efficiency (k_{cat}/K_m), and misincorporation frequency using steady-state kinetic assays (Figure 2B and the Table S2 of the Supporting Information). These parameters allow quanti-

DOI: 10.1021/acs.chemrestox.7b00227
Chem. Res. Toxicol. 2017, 30, 2023−2032

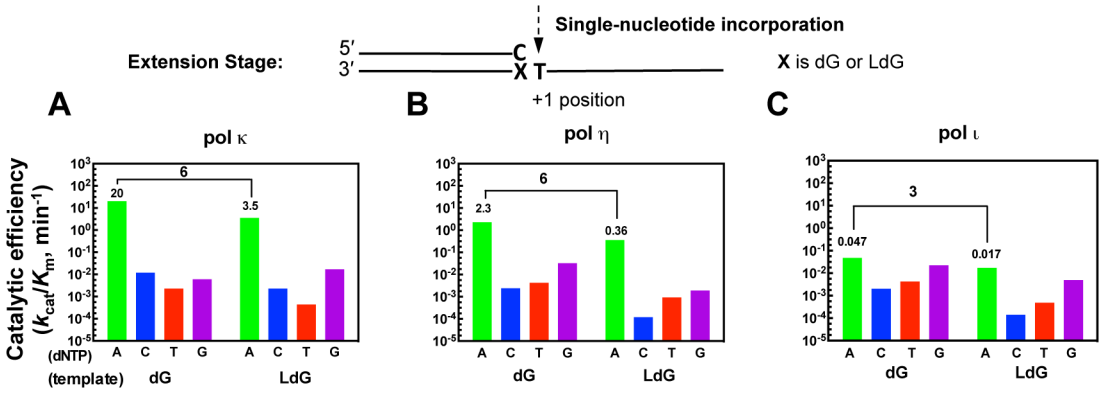

Figure 3. Postlesion extension by human DNA polymerases κ, η, or ι with unmodified or LdG-containing DNA. Catalytic efficiencies of nucleotide incorporations were determined by steady-state kinetic analysis with detailed kinetic parameters shown in the Supporting Information Table S3. Changes in catalytic efficiency relative to a native base pair were calculated from $(k_{cat}/K_{m,dATP})_{unmodified}/(k_{cat}/K_{m,dATP})_{LdG}$ and indicated as x-fold decrease.

Table 1. Summary of Pol κ-Catalyzed Bypass Products from LC−MS/MS Analysis[a]

	5′-...UT 3′-...AA**X**TCACACTGGTCGA	Relative yield of extended products (%)[b]	Nucleotide opposite X
X is dG	TCAGTGTGACCAG	42	dC (error-free)
	TCAGTGTGACCA	58	
X is LdG	TCAGTGTGACCAG	70	dC (error-free)
	TCAGTGTGACCA	30	

[a]X is an unmodified dG or LdG. Percentage of product was calculated on the basis of the peak area in extracted ion chromatograms. The nucleotide incorporated opposite the unmodified dG or LdG lesion is underlined in the extended products. [b]Relative yield of extension products was determined based on the integrated peak areas in extracted ion chromatograms, which were set to extract multiple species with different charged states. The sum of peak area ratios of all products/residual primer was set to 100% for each reaction.

tative assessment of the bypass efficiency and miscoding properties of different enzymes with different DNA and dNTP substrates. As summarized in Figure 2B, the catalytic efficiency of the correct dCTP opposite LdG decreased 10-fold for pol κ, 200-fold for pol η, 70-fold for pol ι, and four-fold for Rev1. Despite the moderate decrease in replication efficiency, pol κ and Rev1 maintained the overall replication fidelity with the LdG-containing DNA substrate. On the contrary, pol η-mediated LdG bypass was error-prone, whereby misincorporations occur more readily (approximately 30−50-fold higher in misincorporation efficiencies) relative to the control DNA. Similarly, the fidelity of DNA replication by pol ι was compromised when replicating past LdG, with dTTP:LdG mispairing occurring at a higher catalytic efficiency than the correct pair, suggesting that pol ι can potentially induce G to A mutations during LdG bypass. The ability of Rev1 to perform dCTP insertion is not significantly perturbed by LdG, judging from the moderate decrease (four-fold) from the catalytic efficiency, which suggests the potential for Rev1 to function redundantly with pol κ for correct dNTP incorporation opposite LdG. Together, these data are consistent with the extension abilities of four polymerases observed in Figure 2A, and demonstrate that dNTP incorporation opposite LdG by major human TLS pols seems to be error-free, especially with pol κ and Rev1.

Postlesion DNA Synthesis Is Mostly Error-Free. The complete bypass of bulky DNA lesions is thought to involve multiple steps by a single or multiple DNA polymerases. The first step is to insert one dNTP opposite the DNA lesion (insertion stage), and the second is to further extend the primer by a few additional dNTPs before a replicative DNA polymerase resumes its function (extension stage).[46,47] On the basis of this two-step bypass model, we further examined the DNA replication fidelity and efficiency at the extension stage. Steady-state kinetic assays were performed with a 16-mer primer annealed to a dG or LdG-containing substrate. The 16-mer primer was designed to have a dCMP at the 3′-end because dCTP was major nucleotide inserted opposite LdG by four TLS pols (Figure 3 and Table S3 of the Supporting Information). We tested the dNTP-incorporation specificity of three pols (pol κ, pol η, and pol ι) that have shown replication activity past the lesion. As shown in Figure 3, in terms of catalytic efficiency of correct nucleotide (dATP), a moderate decrease was observed with all three pols (six-fold for pol κ, six-fold for pol η, and three-fold for pol ι), indicating that LdG does not significantly alter the enzymatic activity at the extension stage. All three polymerase retained the overall fidelity during postlesion synthesis. Our results demonstrate that LdG does not significantly affect the postlesion DNA synthesis *in vitro*, suggesting that three pols tested here can potentially serve as "extender" polymerases. Taking into account these kinetic data and the "two-step, two-polymerase" bypass model, it is likely that both pol κ and Rev1 can insert a dC opposite LdG, and that pol κ, pol η, and pol ι can act redundantly during postlesion extension to achieve error-free bypass.

DOI: 10.1021/acs.chemrestox.7b00227
Chem. Res. Toxicol. 2017, 30, 2023−2032

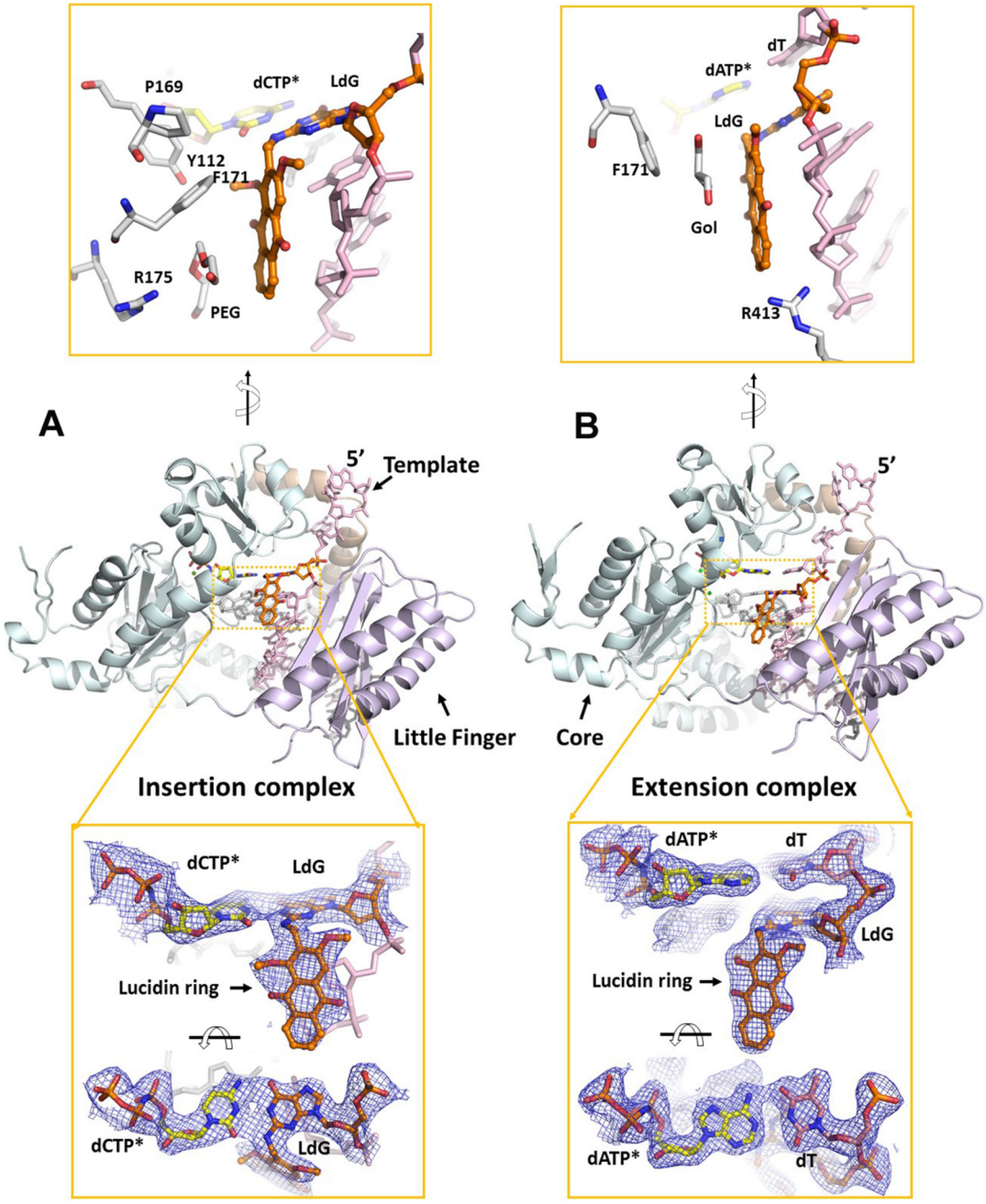

Figure 4. Crystal structures of pol κ: LdG-DNA:dNTP* ternary complexes at the (A) insertion and (B) extension stages. The overall structures of pol κ:LdG-DNA:dNTP* ternary complexes (central panels) are in the back views with the minor groove DNA facing the viewer. dNTP* is dCMPNPP (dCTP*) or dAMPNPP (dATP*). Template is in light pink, primer in gray, LdG in orange, and Mg^{2+} ions in green spheres. The protein is depicted in three colors: core domains (palm, finger and thumb) are in cyan, little finger (LF) is in light purple, and *N*-clasp is in beige. Orthogonal views of the replicating base pairs (bottom panels) at the active site with $2F_o-F_c$ map (blue mesh) contoured at 1σ. Top panels are zoomed-in views of the detailed stabilization of the bulky LdG ring (orange) by surrounding amino acid residues, solvent molecules, polyethene glycol (PEG) and glycerol (Gol), and backbone of the template strand (pink).

Pol κ-Catalyzed Bypass of LdG Is Error-Free As Revealed by LC−MS-Based Oligodeoxynucleotide Sequencing. Pol κ is proficient in DNA synthesis at both insertion and extension stages with LdG adduct as observed in gel electrophoretic analysis (Figure 2A); however, pol κ-mediated TLS is known to generate products containing deletion or frameshift mutations,[48] which cannot be directly observed in the electrophoretic analysis. To detect the potential formation of such erroneous replication products, we used LC−MS/MS-based oligodeoxynucleotide sequencing to determine the sequence and relative yield of products during pol κ-catalyzed DNA synthesis. This method is complementary to the kinetic analysis and is particularly powerful for detecting insertion and deletion mutations.[49,50] As shown in Table 1, translesion synthesis by pol κ past LdG is error-free in the presence of physiological concentrations of nucleotides. The sequence of the oligodeoxynucleotide was obtained from the fragmentation pattern in tandem mass spectrometry analysis (Figures S5 and S6 of the Supporting Information). Major products observed include the cleaved primer (from UDG

DOI: 10.1021/acs.chemrestox.7b00227
Chem. Res. Toxicol. 2017, 30, 2023−2032

digestion and hot piperidine treatment) and the polymerization products. The extended products from an LdG-bearing primer-template DNA are essentially error-free except the relative yields of two products vary slightly from those obtained with a native DNA. The error-free extension by pol κ is consistent with its preference for the correct dNTP incorporation observed in the steady-state kinetic analysis (Figures 2 and 3). Together with the steady-state kinetic analysis, these data demonstrate that pol κ is likely to be an important polymerase for error-free DNA replication and extension beyond lucidin-N^2-dG DNA lesion, although we cannot exclude the potential involvement of other DNA polymerases. Misincorporations caused by translesion synthesis across LdG by major TLS DNA polymerases tested here are T or G by pol η and T by pol ι (Figure 2B and Table S2 of the Supporting Information). These mispairs can potentially lead to G to A transitions and G to C transversions, which have been observed in LuP-treated rats,[16] although they are considered as minor mutations relative to the three major mutations noted earlier.

Structural Basis of Pol κ-Catalyzed LdG Bypass. To gain mechanistic insight into the pol κ-catalyzed LdG bypass, we cocrystallized pol κ with the LdG-adducted DNA substrate and an incoming nucleotide. The first structure (Figure 4A), refined to 2.90 Å resolution, captures pol κ at the insertion stage with LdG pairing with a nonhydrolyzable dCMPNPP (dCTP*). The second structure (Figure 4B), refined to 2.50 Å resolution, represents the extension stage with an incoming dAMPNPP (dATP*) pairing with the 5′-adjacent (of LdG) dTMP. Both ternary complexes are in the same crystal form ($P2_12_12_1$) with two molecules in the asymmetric unit (Table 2), which are isomorphous to the crystals of the pol κ ternary complexes with undamaged DNA (PDB ID: 4U6P) or the BPDE-adducted DNA (PDB IDs: 4U7C, 5T14).[31,32] In the insertion complex, the incoming dCTP* forms a Watson−Crick pair with the template adducted dG (Figure 4A, bottom panel). The distance between the α phosphate of dCTP* and the O atom of 3′−OH of the primer terminal dG is 4.3 Å, indicating a productive conformation for DNA replication at the insertion stage. The lucidin ring of LdG is positioned toward the 3′-end of the template DNA, stabilized by van der Waals interactions with a polyethylene glycol molecule along with several amino acid residues (Tyr 112, Phe 171, Pro169, and Arg175). These van der Waals interactions together shield the hydrophobic lucidin ring from the aqueous solvent. The base pair at the −1 position is tilted due to the presence of LdG at the 0 position, which compromises the stability of DNA at the active site and potentially accounts for the decreased replication activity relative to an unmodified substrate observed in Figure 2B.

In the extension complex, the incoming dATP* pairs with the template dT via canonical Watson−Crick base pairing (Figure 4B, bottom panel). A distance of 4.5 Å between the α phosphate of dATP* and the O atom of 3′−OH of the primer terminal dC suggests a productive conformation for DNA replication at the extension stage. The lucidin ring, a glycerol molecule, and Phe 171 form van der Waals contacts. The presence of LdG at the −1 position does not seem to affect the base pairing at −1 and 0 positions, except that the bulky LdG causes a tilted base pair at the −2 position (Figure 5B, tilted template base in blue relative to the unmodified DNA substrate in gray). Compared to the insertion complex, the replicating base pair (at the 0 position) and its base pair beneath (at the −1 position) form better stacking interactions at the extension stage (Figure 5), potentially alleviating the disrupting effect for DNA replication. This latter observation is consistent with a moderate decrease in catalytic efficiency for pol κ at the extension stage (Figure 3).

Table 2. X-ray Crystallography Data Collection and Refinement Statistics

	pol κ-LdG-dCTP* (insertion) PDB: 5W2A	pol κ-LdG-dATP* (extension) PDB: 5W2C
Data Collection		
space group	$P2_12_12_1$	$P2_12_12_1$
Cell Dimensions		
a, *b*, *c* (Å)	63.9, 129.0, 167.4	63.7, 128.9, 167.7
α, β, γ (deg)	90, 90, 90	90, 90, 90
resolution (Å)[a]	47.3−2.90 (3.06−2.90)	50.00−2.50 (2.64−2.50)
R_{merge} (%)	5.6 (57.8)	4.4 (47.7)
$I/\sigma I$	14.8 (2.5)	16.3 (2.7)
completeness (%)	99.2 (99.8)	99.5 (99.7)
redundancy	4.8 (5.0)	4.4 (4.5)
Refinement		
resolution (Å)	47.3−2.9	50.0−2.50
no. reflns	29 905	47 145
R_{work}/R_{free} (%)	23.1/26.9	21.1/25.3
No. Atoms		
protein	6663	6717
DNA	942	932
ligand	56	60
water	28	213
Avg. *B*-Factors (Å²)		
protein	113.2	84.5
DNA	105.6	74.5
ligand	95.4	61.2
water	79.2	68.3
r.m.s.d.		
bond lengths (Å)	0.009	0.009
bond angles (deg)	1.4	1.4

[a]Values in parentheses are for the highest resolution shell.

The key structural component of pol κ is the open active-site cleft at the minor groove side of substrate DNA (Figure 4), which accommodates the lucidin ring (or the BPDE ring as observed previously[31,32]). This structural feature of pol κ keeps the DNA substrate in the standard B-form (Figure 5, right panels), judging from the superimposed structures of LdG-DNA and the unmodified, B-form DNA from another pol κ structure.[44] Indeed, pol κ maintains the same conformation in a number of solved ternary complexes regardless of different DNA substrates; structural comparisons using root-mean-square deviations are shown in Table S4 of the Supporting Information. The presence of the open active-site cleft is consistent with the ability of pol κ to accommodate an array of DNA lesions.[31,41−44] The lucidin ring of LdG is positioned toward the 3′-end of the template DNA, consistent with the orientation predicted using the molecular dynamic simulations.[23] Collectively, these structural data shed light on the mechanism of pol κ-mediated LdG bypass.

The replication-blocking and mutagenic properties of bulky DNA lesions are attributed in part to the difficulty for DNA polymerases to accommodate these modifications at the enzyme active site.[51] For replicative DNA polymerases, the DNA minor groove is enclosed by surrounding amino acid

DOI: 10.1021/acs.chemrestox.7b00227
Chem. Res. Toxicol. 2017, 30, 2023−2032

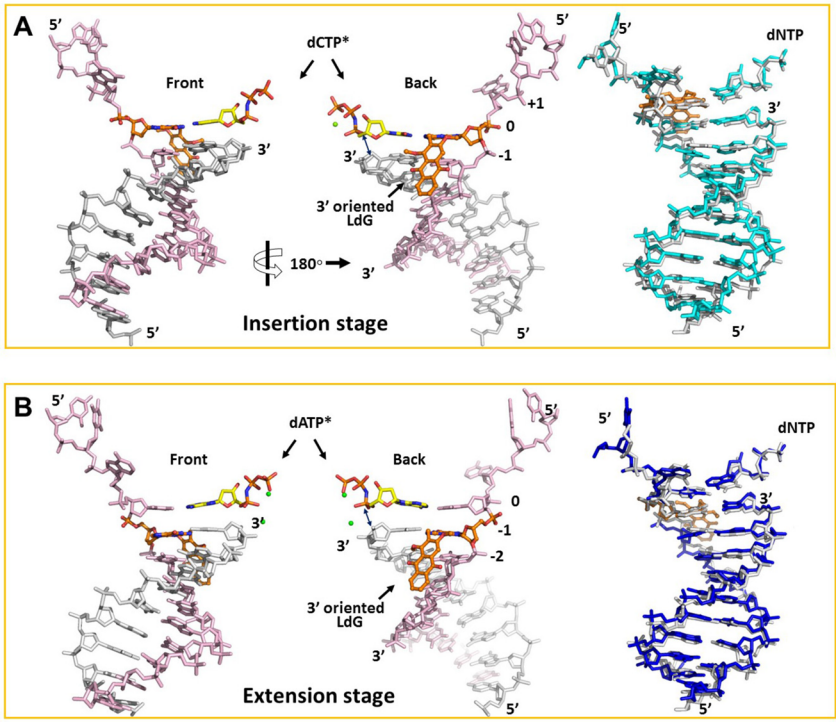

Figure 5. Structures of LdG-harboring DNA within pol κ-bound complexes at the (A) insertion and (B) extension stages. The color scheme of the left and middle panels is the same as described in Figure 4. Incoming dNTP* is in yellow, where dNTP* is dCMPNPP (dCTP*) or dAMPNPP (dATP*). The double arrowed lines illustrate a distance of 4.3−4.5 Å between the 3′−OH of the primer and the α phosphate of dNTP*. In both insertion and extension complexes, the lucidin ring is oriented toward the 3′-end of the template strand. The right panels illustrate the superposition of LdG-containing DNA with unmodified DNA in a pol κ complex (PDB codes: 2OHO). The unmodified DNA is in gray and the adducted DNA (LdG adduct in orange) is in cyan (insertion stage) and blue (extension stage).

residues at the active site,[52−54] which explains why LdG is a potent inhibitor for DNA synthesis by Klenow fragment.[23] On the other hand, most Y-family DNA polymerases, such as pol η and pol ι, have a narrow opening at the substrate DNA minor groove, likely to be insufficient to house the lucidin ring. Our observation that LdG drastically reduces the replication efficiency of pol η and pol ι is consistent with this notion (Figure 2B). Modeling BPDE-N^2-dG adduct (also a bulky N^2-dG adduct) to the active sites of pol η and pol ι results in steric clash, which further confirms the incompetency of these pols in bypass bulky N^2-dG adducts.[31,37] Another model Y-family DNA polymerase, *Sulfolobus solfataricus* P2 DNA polymerase IV (Dpo4), excludes the bulky BPDE ring out of the active site due to the lack of space.[55] However, such relocation of bulky lesions destabilizes the double helical DNA structure and introduces misinsertions during replication.[55]

CONCLUSION

In conclusion, we have obtained the first set of biochemical and structural data to elucidate the miscoding property of lucidin-N^2-dG DNA lesion with human enzymes. Our results demonstrate that DNA replication past the LdG is largely error-free with four human TLS pols examined. In addition, two X-ray crystal structures of pol κ provide mechanistic insights into the error-free LdG bypass catalyzed by pol κ. Together, these data support the low carcinogenic risk of madder root in humans. We reason that lucidin-N^2-dG DNA lesion can be repaired efficiently or bypassed largely error-free by pol κ in humans. Future biological studies are warranted to further illuminate these points.

ASSOCIATED CONTENT

Supporting Information

The Supporting Information is available free of charge on the ACS Publications website at DOI: 10.1021/acs.chemrestox.7b00227.

Procedures for preparing LdG-harboring oligodeoxynucleotides; steady-state kinetic parameters; mass spectrometric data (PDF)

Accession Codes

Coordinates and structure factors for the insertion complex (5W2A) and the extension complex (5W2C) have been deposited in the Protein Data Bank.

AUTHOR INFORMATION

Corresponding Authors

*E-mail: linlin.zhao@cmich.edu. Phone: (989) 774-3252. Fax: (989) 774-3883.
*E-mail: pradeep@chem.iitb.ac.in.
*E-mail: hling4@uwo.ca.

ORCID

P. I. Pradeepkumar: 0000-0001-9104-3708
Linlin Zhao: 0000-0002-8821-4198

Author Contributions

¶These authors contributed equally to this work.

Funding

This project is supported in part by US National Institutes of Health Grant No. R15 GM117522 (to L.Z.), Central Michigan University start-up funds (to L.Z.), Canadian Institutes of Health Research Operating Grant No. MOP-67128 (to H.L.),

DOI: 10.1021/acs.chemrestox.7b00227
Chem. Res. Toxicol. 2017, 30, 2023−2032

and Department of Biotechnology (DBT)-Government of India Grant No. BT/PR8265/BRB/10/1228/2013 (to P.I.P.). Use of the Advanced Photon Source, an Office of Science User Facility operated for the U.S. Department of Energy (DOE) Office of Science by Argonne National Laboratory, is supported by the U.S. DOE under Contract No. DE-AC02−06CH11357. The content is solely the responsibility of the authors and does not necessarily represent the official views of the National Institutes of Health.

Notes

The authors declare no competing financial interest.

■ ACKNOWLEDGMENTS

We thank the staff at the beamline 24ID of the Advance Photon Source (APS) for data collection.

■ ABBREVIATIONS

BPDE, benzo[*a*]pyrene-7,8-dihydrodiol-9,10-epoxide; dAMPNPP, 2′-deoxyadenosine-5′-[(α,β)-imido] triphosphate; dCMPNPP, 2′-deoxycytidine-5′-[(α,β)-imido] triphosphate; LdG, N^2-methyl-(1,3-dimethoxyanthraquinone)-deoxyguanosine; LuP, lucidin-3-*O*-primeveroside; N^6-dA, N^6-2′-deoxyadenosine; N^2-dG, N^2-2′-deoxyguanosine; pol, DNA polymerase; UDG, uracil DNA glycosylase

■ REFERENCES

(1) Poirier, M. C., Santella, R. M., and Weston, A. (2000) Carcinogen macromolecular adducts and their measurement. *Carcinogenesis 21*, 353−359.
(2) Hecht, S. S. (2003) Tobacco carcinogens, their biomarkers and tobacco-induced cancer. *Nat. Rev. Cancer 3*, 733−744.
(3) Poirier, M. C. (2004) Chemical-induced DNA damage and human cancer risk. *Nat. Rev. Cancer 4*, 630−637.
(4) Balbo, S., Turesky, R. J., and Villalta, P. W. (2014) DNA adductomics. *Chem. Res. Toxicol. 27*, 356−366.
(5) Hoeijmakers, J. H. J. (2001) Genome maintenance mechanisms for preventing cancer. *Nature 411*, 366−374.
(6) Yang, W., and Woodgate, R. (2007) What a difference a decade makes: insights into translesion DNA synthesis. *Proc. Natl. Acad. Sci. U. S. A. 104*, 15591−15598.
(7) Sale, J. E. (2013) Translesion DNA synthesis and mutagenesis in eukaryotes. *Cold Spring Harbor Perspect. Biol. 5*, a012708.
(8) Waters, L. S., Minesinger, B. K., Wiltrout, M. E., D'Souza, S., Woodruff, R. V., and Walker, G. C. (2009) Eukaryotic translesion polymerases and their roles and regulation in DNA damage tolerance. *Microbiol. Mol. Biol. Rev. 73*, 134−154.
(9) Lange, S. S., Takata, K.-i., and Wood, R. D. (2011) DNA polymerases and cancer. *Nat. Rev. Cancer 11*, 96−110.
(10) Zhang, Y., Yuan, F., Wu, X., Wang, M., Rechkoblit, O., Taylor, J.-S., Geacintov, N. E., and Wang, Z. (2000) Error-free and error-prone lesion bypass by human DNA polymerase κ in vitro. *Nucleic Acids Res. 28*, 4138−4146.
(11) Avkin, S., Goldsmith, M., Velasco-Miguel, S., Geacintov, N., Friedberg, E. C., and Livneh, Z. (2004) Quantitative analysis of translesion DNA synthesis across a benzo[*a*]pyrene-guanine adduct in mammalian cells: the role of DNA polymerase κ. *J. Biol. Chem. 279*, 53298−53305.
(12) Westendorf, J., Marquardt, H., Poginsky, B., Dominiak, M., Schmidt, J., and Marquardt, H. (1990) Genotoxicity of naturally occurring hydroxyanthraquinones. *Mutat. Res., Genet. Toxicol. Test. 240*, 1−12.
(13) Poginsky, B., Westendorf, J., Blömeke, B., Marquardt, H., Hewer, A., Grover, P. L., and Phillips, D. H. (1991) Evaluation of DNA-binding activity of hydroxyanthraquinones occurring in Rubia tinctorum L. *Carcinogenesis 12*, 1265−1271.
(14) (2000) *PDR for Herbal Medicines*, Medical Economics Co., Montvale, NJ.
(15) Nohmi, T., Masumura, K., and Toyoda-Hokaiwado, N. (2017) Transgenic rat models for mutagenesis and carcinogenesis. *Genes and Environment 39*, 11.
(16) Umemura, T. (2014) Possible Carcinogenic Mechanisms Underlying Renal Carcinogens in Food. *Food Safety 2*, 17−30.
(17) Inoue, K., Yoshida, M., Takahashi, M., Shibutani, M., Takagi, H., Hirose, M., and Nishikawa, A. (2009) Induction of kidney and liver cancers by the natural food additive madder color in a two-year rat carcinogenicity study. *Food Chem. Toxicol. 47*, 184−191.
(18) Ishii, Y., Takasu, S., Kuroda, K., Matsushita, K., Kijima, A., Nohmi, T., Ogawa, K., and Umemura, T. (2014) Combined application of comprehensive analysis for DNA modification and reporter gene mutation assay to evaluate kidneys of gpt delta rats given madder color or its constituents. *Anal. Bioanal. Chem. 406*, 2467−2475.
(19) (2002) Some traditional herbal medicines, C. *Rubia tinctorum*, *Morinda officinalis*, and anthraquinones. In *IARC Monographs on the Evaluation of Carcinogenic Risks to Humans. Some Traditional Herbal Medicines, Some Mycotoxins, Naphthalene, and Styrene*, pp 129−151, IARC Press, Lyon, France.
(20) Ishii, Y., Okamura, T., Inoue, T., Fukuhara, K., Umemura, T., and Nishikawa, A. (2010) Chemical Structure Determination of DNA Bases Modified by Active Metabolites of Lucidin-3-*O*-primeveroside. *Chem. Res. Toxicol. 23*, 134−141.
(21) Ishii, Y., Inoue, K., Takasu, S., Jin, M., Matsushita, K., Kuroda, K., Fukuhara, K., Nishikawa, A., and Umemura, T. (2012) Determination of lucidin-specific DNA adducts by liquid chromatography with tandem mass spectrometry in the livers and kidneys of rats given lucidin-3-*O*-primeveroside. *Chem. Res. Toxicol. 25*, 1112−1118.
(22) Inoue, K., Yoshida, M., Takahashi, M., Fujimoto, H., Ohnishi, K., Nakashima, K., Shibutani, M., Hirose, M., and Nishikawa, A. (2009) Possible contribution of rubiadin, a metabolite of madder color, to renal carcinogenesis in rats. *Food Chem. Toxicol. 47*, 752−759.
(23) Ghodke, P. P., Harikrishna, S., and Pradeepkumar, P. I. (2015) Synthesis and Polymerase-Mediated Bypass Studies of the N 2-Deoxyguanosine DNA Damage Caused by a Lucidin Analogue. *J. Org. Chem. 80*, 2128−2138.
(24) Pence, M. G., Choi, J. Y., Egli, M., and Guengerich, F. P. (2010) Structural basis for proficient incorporation of dTTP opposite O6-methylguanine by human DNA polymerase iota. *J. Biol. Chem. 285*, 40666−40672.
(25) Choi, J.-Y., and Guengerich, F. P. (2005) Adduct size limits efficient and error-free bypass across bulky N^2-guanine DNA lesions by human DNA polymerase η. *J. Mol. Biol. 352*, 72−90.
(26) Zhao, L., Pence, M. G., Eoff, R. L., Yuan, S., Fercu, C. A., and Guengerich, F. P. (2014) Elucidation of kinetic mechanisms of human translesion DNA polymerase κ using tryptophan mutants. *FEBS J. 281*, 4394−4410.
(27) Swan, M. K., Johnson, R. E., Prakash, L., Prakash, S., and Aggarwal, A. K. (2009) Structure of the Human Rev1-DNA-dNTP Ternary Complex. *J. Mol. Biol. 390*, 699−709.
(28) Xu, W., Ouellette, A. M., Wawrzak, Z., Shriver, S. J., Anderson, S. M., and Zhao, L. (2015) Kinetic and structural mechanisms of (5′*S*)-8,5′-cyclo-2′-deoxyguanosine-induced DNA replication stalling. *Biochemistry 54*, 639−651.
(29) Traut, T. W. (1994) Physiological concentrations of purines and pyrimidines. *Mol. Cell. Biochem. 140*, 1−22.
(30) Rozenski, J., and McCloskey, J. A. (2002) SOS: A simple interactive program for ab initio oligonucleotide sequencing by mass spectrometry. *J. Am. Soc. Mass Spectrom. 13*, 200−203.
(31) Jha, V., Bian, C., Xing, G., and Ling, H. (2016) Structure and mechanism of error-free replication past the major benzo[*a*]pyrene adduct by human DNA polymerase κ. *Nucleic Acids Res. 44*, 4957−4967.
(32) Jha, V., and Ling, H. (2017) Structural basis of accurate replication beyond a bulky major benzo[*a*]pyrene adduct by human DNA polymerase kappa. *DNA Repair 49*, 43−50.

DOI: 10.1021/acs.chemrestox.7b00227
Chem. Res. Toxicol. 2017, 30, 2023−2032

(33) Winn, M. D., Ballard, C. C., Cowtan, K. D., Dodson, E. J., Emsley, P., Evans, P. R., Keegan, R. M., Krissinel, E. B., Leslie, A. G., McCoy, A., McNicholas, S. J., Murshudov, G. N., Pannu, N. S., Potterton, E. A., Powell, H. R., Read, R. J., Vagin, A., and Wilson, K. S. (2011) Overview of the CCP4 suite and current developments. *Acta Crystallogr., Sect. D: Biol. Crystallogr. 67*, 235−242.
(34) Murshudov, G. N., Vagin, A. A., and Dodson, E. J. (1997) Refinement of macromolecular structures by the maximum-likelihood method. *Acta Crystallogr., Sect. D: Biol. Crystallogr. 53*, 240−255.
(35) Emsley, P., and Cowtan, K. (2004) Coot: model-building tools for molecular graphics. *Acta Crystallogr., Sect. D: Biol. Crystallogr. 60*, 2126−2132.
(36) DeLano, W. L. (2002) *The PyMOL Molecular Graphics System*; DeLano Scientific, San Carlos, CA. http://www.pymol.org (accessed 6/30/2017).
(37) Zhao, L., and Washington, T. M. (2017) Translesion Synthesis: Insights into the Selection and Switching of DNA Polymerases. *Genes 8*, 24.
(38) Waters, L. S., and Walker, G. C. (2006) The critical mutagenic translesion DNA polymerase Rev1 is highly expressed during G_2/M phase rather than S phase. *Proc. Natl. Acad. Sci. U. S. A. 103*, 8971−8976.
(39) Fuchs, R. P. (2016) Tolerance of lesions in E. coli: Chronological competition between Translesion Synthesis and Damage Avoidance. *DNA Repair 44*, 51−58.
(40) Indiani, C., and O'Donnell, M. (2013) A proposal: Source of single strand DNA that elicits the SOS response. *Front. Biosci., Landmark Ed. 18*, 312.
(41) Choi, J.-Y., Angel, K. C., and Guengerich, F. P. (2006) Translesion synthesis across bulky N2-alkyl guanine DNA adducts by human DNA polymerase κ. *J. Biol. Chem. 281*, 21062−21072.
(42) Irimia, A., Eoff, R. L., Guengerich, F. P., and Egli, M. (2009) Structural and functional elucidation of the mechanism promoting error-prone synthesis of human DNA polymerase K opposite the 7,8-dihydro-8-oxodeoxyguanosine adduct. *J. Biol. Chem. 284*, 22467−22480.
(43) Carpio, R. V.-D., Silverstein, T. D., Lone, S., Swan, M. K., Choudhury, J. R., Johnson, R. E., Prakash, S., Prakash, L., and Aggarwal, A. K. (2009) Structure of Human DNA Polymerase κ Inserting dATP Opposite an 8-OxoG DNA Lesion. *PLoS One 4*, e5766.
(44) Lone, S., Townson, S. A., Uljon, S. N., Johnson, R. E., Brahma, A., Nair, D. T., Prakash, S., Prakash, L., and Aggarwal, A. K. (2007) Human DNA polymerase kappa encircles DNA: implications for mismatch extension and lesion bypass. *Mol. Cell 25*, 601−614.
(45) Frank, E. G., and Woodgate, R. (2007) Increased catalytic activity and altered fidelity of human DNA polymerase ι in the presence of manganese. *J. Biol. Chem. 282*, 24689−24696.
(46) Shachar, S., Ziv, O., Avkin, S., Adar, S., Wittschieben, J., Reißner, T., Chaney, S., Friedberg, E. C., Wang, Z., Carell, T., Geacintov, N., and Livneh, Z. (2009) Two-polymerase mechanisms dictate error-free and error-prone translesion DNA synthesis in mammals. *EMBO J. 28*, 383−393.
(47) Livneh, Z., Z, O., and Shachar, S. (2010) Multiple two-polymerase mechanisms in mammalian translesion DNA synthesis. *Cell Cycle 9*, 729−735.
(48) Mukherjee, P., Lahiri, I., and Pata, J. D. (2013) Human polymerase kappa uses a template-slippage deletion mechanism, but can realign the slipped strands to favour base substitution mutations over deletions. *Nucleic Acids Res. 41*, 5024−5035.
(49) Chowdhury, G., and Guengerich, F. P. (2011) Liquid Chromatography-Mass Spectrometry Analysis of DNA Polymerase Reaction Products. In *Current Protocols in Nucleic Acid Chemistry*, Suppl. 47, John Wiley & Sons, Inc.
(50) Xu, W., Ouellette, A., Ghosh, S., O'Neill, T. C., Greenberg, M. M., and Zhao, L. (2015) Mutagenic bypass of an oxidized abasic lesion-induced DNA interstrand cross-link analogue by human translesion synthesis DNA polymerases. *Biochemistry 54*, 7409−7422.
(51) Geacintov, N. E., Cosman, M., Hingerty, B. E., Amin, S., Broyde, S., and Patel, D. J. (1997) NMR solution structures of stereoisomeric covalent polycyclic aromatic carcinogen-DNA adducts: principles, patterns, and diversity. *Chem. Res. Toxicol. 10*, 111−146.
(52) Doublié, S., Tabor, S., Long, A. M., Richardson, C. C., and Ellenberger, T. (1998) Crystal structure of a bacteriophage T7 DNA replication complex at 2.2 Å resolution. *Nature 391*, 251−258.
(53) Franklin, M. C., Wang, J., and Steitz, T. A. (2001) Structure of the replicating complex of a pol α family DNA polymerase. *Cell 105*, 657−667.
(54) Steitz, T. A. (1999) DNA polymerases: structural diversity and common mechanisms. *J. Biol. Chem. 274*, 17395−17398.
(55) Bauer, J., Xing, G., Yagi, H., Sayer, J. M., Jerina, D. M., and Ling, H. (2007) A structural gap in Dpo4 supports mutagenic bypass of a major benzo[*a*]pyrene dG adduct in DNA through template misalignment. *Proc. Natl. Acad. Sci. U. S. A. 104*, 14905−14910.

DOI: 10.1021/acs.chemrestox.7b00227
Chem. Res. Toxicol. 2017, 30, 2023−2032